Since January 2020 Elsevier has created a COVID-19 resource centre with free information in English and Mandarin on the novel coronavirus COVID-19. The COVID-19 resource centre is hosted on Elsevier Connect, the company's public news and information website.

CHAPTER 1

Spatiotemporal dynamics of the first wave of the COVID-19 epidemic in Brazil

J.M.V. Grzybowski[a], **R.V. da Silva**[a], **and M. Rafikov**[b]

[a] *Federal University of Fronteira Sul, Erechim, RS, Brazil* [b] *Center for Engineering, Modeling and Applied Social Sciences (CECS), Federal University of ABC (UFABC), Santo André, São Paulo, Brazil*

1.1 Introduction

The first wave of the COVID-19 epidemic left a considerable trail of changes as it swept through countries with enormous volume and velocity. Enormous volumes of data and research have been generated in attempts to break the transmission chains, flatten the curve, and better the survival rates. As the first wave recedes and most countries are believed to remain vulnerable to a second wave, it is time to gain insights that help avoid it or at least mitigate it as much as possible. Most of the discussions regarding strategies to fight the pandemic apply results from mathematical models, which have driven policies and substantially oriented governmental decisions [1,2].

In this context, the reproduction number is the single most relevant parameter applied to analyze the development and evolution of the epidemic. It is defined as the average number of new infections caused by an infected individual during the infectious time window [3]. The initial reproduction number (when almost the entire population is susceptible) is termed basic reproduction number, R_0, whereas the reproduction number under a lesser number of susceptible individuals is termed effective reproduction number, R_e. The most common approach to deal with epidemic modeling is to regard the reproduction number as a constant during the evolution of the epidemic [4–13]. This illustrates the situation of an epidemic outbreak in which specific control measures are not taken or are not effective whatsoever. Nevertheless, in the case of COVID-19, control measures effectively worked to change the aspect of epidemic curves, to the point that several countries had the first wave of the epidemic controlled by drastically reducing the reproduction number. Thus, even not having acquired a herd immunity status, they managed to extinguish the conditions that would sustain the epidemic, at least temporarily, by reducing the value of the reproduction number, to which we will refer as time-varying reproduction number R_t following previous publications [3,14].

Mathematical Analysis of Infectious Diseases
https://doi.org/10.1016/B978-0-32-390504-6.00006-1

In practice, under the COVID-19 epidemic, the application of constant reproduction numbers results in a cumbersome process because they can hardly calibrate the model to data, except for very initial stages of the epidemic. For this reason, the application of phase-adjusted or time-varying reproduction numbers has appeared more strongly in recent publications [3,15–17]. Not only time-varying reproduction numbers provide better model calibration, but also they give a more realistic prognostic. Recall that early prognostic of confirmed cases and death tolls due to the COVID-19, obtained by means of models with constant reproduction numbers, can now be seen as visibly overrated estimates that reflect the difficulty of capturing the dynamics of the epidemic by means of a constant reproduction coefficient [18].

Monitoring the time-varying reproduction allows one to trace the status of disease spread and also the conditions under which the epidemic state sets in. As a disease with rapidly growing contagion curve and as a consequence of rapid changes in the social distancing policies and their effectiveness, the time-varying reproduction number can feature very heterogeneous behavior across a continent-wide country. Where did it start and then where it headed to? What is the maximum value of the reproduction number in a given area? How is the temporal profile of R_t related to variables such as HDI (Human Development Index) and demographic density? What are the main contagion pathways to the rapid dissemination of the virus? As the first wave of the epidemic in Brazil started to recede, a massive amount of data became available. This enables the evaluation of spatiotemporal aspects of the epidemic in such a way that both geographical and temporal aspects are taken into account in an integrated way. The results can help unveil some relevant knowledge about the virtues and vices of policies and decisions affected in Brazil since the beginning of the pandemic and shed some light into these and other questions.

We collected time series data from over 5570 Brazilian cities and provided a countrywide spatiotemporal analysis of the characteristics of the first wave of COVID-19 in Brazil. The insights obtained by means of this study include the understanding of the likely pathways of transmission and of the dynamics of the hot spots of contagion over time. The knowledge of such traits can be applied in a potential second wave to counteract the effects of organic contagion pathways and more effectively break likely interregional transmission chains at early stages. In this context, the reproduction number allows establishing the status of the epidemic over time, acquiring prognostics and scenarios, and evaluating the effectiveness of social distancing measures over time. The results of this study agree with those of previous publications carried out using different methodologies in the sense that COVID-19 containment measures were late [19,20].

1.2 Materials and methods

This section starts by presenting the SEIR model applied in the study and the calibration procedure. The calibration was performed to determine the time-varying instantaneous number, which is the most important parameter to characterize the epidemic. In particular, we pay attention to the transition from the epidemic-free state to the epidemic state, which corresponds to the moment when the time-varying reproduction number features a low-high transition that crosses $R_t = 1$. The transition edge is properly identified by means of a Green-Reds colormap. Further, we briefly present some important aspects of Brazil, such as demographic density, DHI, which may partially respond to questions regarding the effectiveness of social distancing measures. Additionally, we present the air transport network, which allows us to evaluate the hypothesis that early dissemination of the virus through the country is strongly associated with the circulation of air passengers.

1.2.1 The SEIR model

The SEIR model stratifies a population N into four compartments, namely: Susceptible (S), Exposed (E), Infected (I), and Removed (R). The interrelations among the compartments can be described in the form of a system of four first-order autonomous differential equations

$$\begin{aligned} \frac{dS}{dt} &= -\frac{\beta_t}{N} SI \\ \frac{dE}{dt} &= \frac{\beta_t}{N} SI - \sigma E \\ \frac{dI}{dt} &= \sigma E - \gamma I \\ \frac{dR}{dt} &= \gamma I, \end{aligned} \tag{1.1}$$

where $\beta_t = \gamma R_t$, R_t is the instantaneous transmission rate, γ^{-1} is the average duration of the infection, and σ^{-1} is the average incubation time of the infection. The total population under consideration, N, is given by

$$N = S + E + I + R. \tag{1.2}$$

Meanwhile, R_t is the parameter of the model depending of social behavior and calibrated to the time series of confirmed cases obtained from State Health Secretaries from each Brazilian state.

Table 1.1: Parameters applied in the study and their sources.

Parameter	Value	95% CI	Reference
σ^{-1}	5.2	4.1–7.0	Li et al. [21]
γ^{-1}	10.5	9.0–12.0	NCID [22]

Estimated on the basis of the evidences presented in the publication by NCID [22]. Meanwhile, You et al. [3] consider the infectious period to last in average 13.91 days.

1.2.2 Model integration

The model was integrated using the Fourth-order Runge-Kutta method with integration step $h = 1$ day. The computer simulations were performed in an Intel i7-7700 CPU at 3.60 Ghz with a 6 GB NVIDIA GeForce GTX 1060 video card. All the computer routines were developed using Python 3.7 language. The parameters σ^{-1} and γ^{-1} were defined as normal probability distributions with mean and standard deviation as given in Table 1.1. From these distributions, 10,000 simulations were performed. Each plot shows the mean value of all the simulations and lower/upper buffers for a 95% confidence interval.

1.2.3 Model calibration

It is widely recognized that official data on the COVID-19 epidemic are hampered by sources of uncertainty, such as time-varying undertesting, lag in the publication of test results, lack of accuracy in infection dating, and the so-called 'Monday dip', which is a weekly pattern of reduction in the number of confirmed cases and deaths, presumably due to the reduced working regime of laboratories on weekends. Furthermore, many of the research data are preliminary in the sense that they come from data sources that prioritize agility in the publication of data that are likely to be revised and consolidated in the future. Thus, for now, the calibration of epidemic models based on confirmed infection data can lead to highly inaccurate prognostics.

To avoid the direct calibration of the model with the time series data from confirmed cases and deaths, we first apply the data to calibrate a logistic function and then apply the output of the logistic function to calibrate the SEIR model. Notice that official COVID-19 data are commonly presented or transformed into time series of a cumulative number of confirmed cases and a cumulative number of deaths. The characteristic of the COVID-19 epidemic of providing lasting immunity to recovered individuals makes the curve of the confirmed cases have the S-shaped curve. As such, the process of model calibration involved two main steps: (i) calibration of the logistic equation, a much simpler model, to the confirmed cases data, and (ii) calibration of the SEIR model to the output of the calibrated logistic equation.

The logistic equation is a first-order autonomous differential equation given by

$$\frac{dx}{dt} = rx\left(1 - \frac{x}{K}\right), \tag{1.3}$$

where r is the growth rate and K is the carrying capacity. The logistic equation admits an analytical solution, which is given by

$$x(t) = \frac{Kx_0}{x_0 + (K - x_0)\,e^{-rt}}. \tag{1.4}$$

The model calibration focused on three parameters: the time-varying instantaneous number, R_t, the incubation period, σ^{-1}, and the infectious period, γ^{-1}. The time-varying instantaneous reproduction number, R_t, reflects social behavior and is derived by fitting the dynamical evolution of the sum of infected and removed individuals ($I + R$) to time series data of confirmed cases. As social behavior changes over time for several reasons related to the epidemic, seek for a time-varying R_t that best fits the model outputs to the data at each integration step. Meanwhile, σ^{-1} and γ^{-1} are clinical parameters presented in the literature as normal distributions represented by the mean and standard deviation. They are represented as such in the model input such that the integration is performed by means of a Monte-Carlo process. As a consequence, the time-varying profile of R_t is obtained within such a range of uncertainties in the input parameters. The best fit of the model to data in each case is chosen by means of the minimum of the Root Mean Squared Error (RMSE).

1.2.4 Parameters

Clinical parameters applied in the model such as σ^{-1} and γ^{-1} were adopted from clinical studies. The parameter values are shown in Table 1.1.

1.2.5 Case study: Brazil

The territorial extension of Brazil is 8.5 million km^2, approximately, thus the largest country in South America and the fifth in the world. It borders the following countries: French Guiana, Suriname, Guyana, Venezuela, and Colombia to the North; Peru, Bolivia, Paraguay, and Argentina to the West; and Uruguay to the South. Brazil's political-administrative division is organized in 26 states and one federal district, which are distributed in five geographical regions (North, Northeast, Central-West, Southeast, and South), as shown in Fig. 1.1. According to the latest annual revision of territorial areas and borders [23], Brazil has 5568 municipalities, plus the island district of Fernando de Noronha and the Federal District.

Figure 1.1: Brazil and its states and state capital cities.

According to the World Bank population projection for 2019 [24], Brazil occupies the 6th position with 211,049.53 thousand inhabitants. The demographic density in the country is quite diverse, with values ranging from 0.1 to 13 thousand inhabitants per km^2, approximately [25]. Fig. 1.2a depicts the spatial distribution of the demographic density. It is noticeable that the South, Southeast, and littoral of Northeast regions concentrate the higher densities. It is worth mentioning the municipality of Manaus (state of Amazonas – AM) in the North region, which has the highest demographic density of the region, with approximately 158 inhabitants per km^2. The metropolitan areas of São Paulo (SP) and Rio de Janeiro (RJ) cities in the Southeast region have the highest demographic densities of the country, with values of 12.5 to 13 thousand inhabitants per km^2, approximately. Still regarding high demographic density, one may highlight the cities of Porto Alegre (RS) and Curitiba (PR) in the South region, the Federal District (DF) in the Central-West region, the cities of Salvador (BA), Aracaju (SE), Maceió (AL), Recife (PE), João Pessoa (PB), Natal (RN), and Fortaleza (CE) in the Northeast region.

In terms of economy, Brazil's 2019 Gross Domestic Product (GDP) figures among the top 10 countries, more precisely, in the 9th position. In contrast, regarding the global ranking on the GPD per capita, the country is in the 95th position [26,27]. Conversely, the country occupies the 75th position on the Human Development Index (HDI) (0.761) [28]. At the municipalities' level, the distribution of the HDI is also heterogeneous. Fig. 1.2b shows the distribution of the

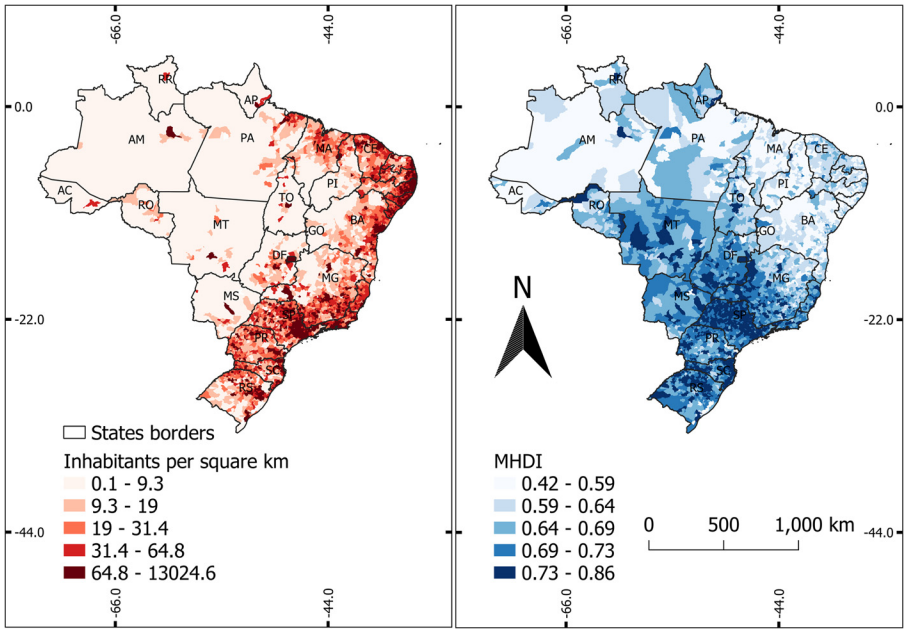

Figure 1.2: Brazil in terms of (a) demographic density and (b) Human Development Index.

municipal HDI. Higher values of HDI occurred in the South and Southeast regions, with values up to 0.862. The municipalities of Manaus and Porto Velho stand out in the North region with HDI values of 0.737 and 0.736, respectively [29].

Brazil, with its vast territorial area and long distances between cities, relies on air transportation, which is well developed. The country holds the 10th position in the global ranking on the number of passengers carried [30]. Fig. 1.3 shows the air links among the main cities in Brazil. The airports in São Paulo (Guarulhos International Airport) and Rio Janeiro cities (Galeão International Airport) get most of the international flights. Thus, these two airports become the central air hubs to distribute domestic flights throughout the country. These two airports, together with the airports located in the cities of Porto Alegre (RS), Curitiba (PR), Brasília (DF), Belo Horizonte (MG), and Salvador (BA), formed the air links in charge of the transportation of 1.7 to 5.7 million passengers per year [31].

Data on the Covid-19 pandemic in Brazil were acquired from Brasil.io repository [32]. It is an online platform that counts with 40 volunteers for data compilation from the 27 Health State Secretaries.

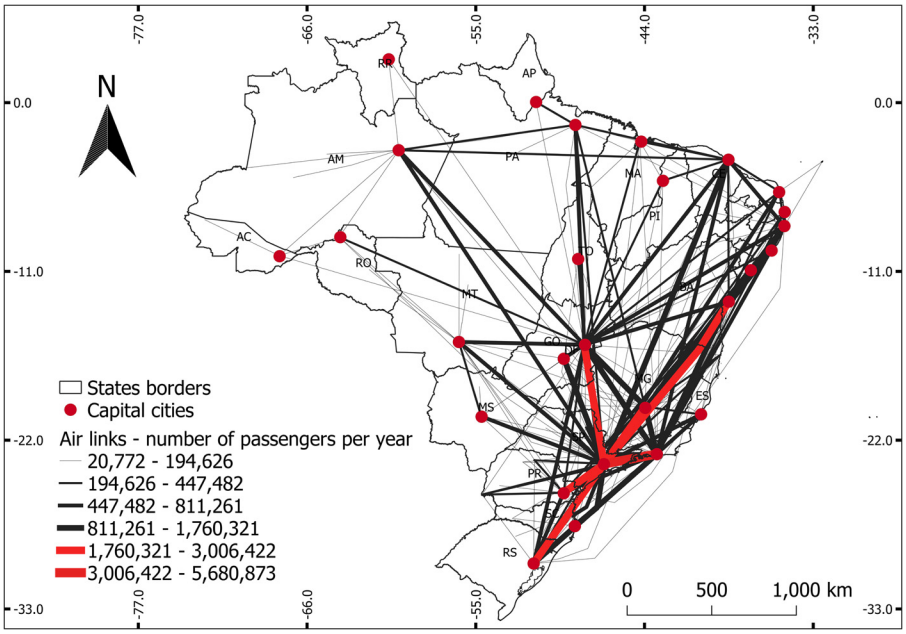

Figure 1.3: Air transportation network in Brazil in terms of the number of passengers per year.

1.2.6 Obtaining a network structure from R_t data

To obtain a network structure that may help visualize the early transmission network of COVID-19, we implement a simple algorithm to generate nodes and edges. To generate the network nodes, we will consider the R_t profile of the first three epidemiological weeks in Brazil, which correspond to EW 9 to EW 11. Municipalities entering the epidemic state $R_t > 1$ during this time window will be regarded as nodes of the early transmission network. In turn, the edges will be generated on the basis of two important metrics that permeate the study of spatio-temporal networks (STN) are travel distances and travel times.

Denote as N_L the number of locations entering epidemic state during such period and consider i as an arbitrary index that we define to number the nodes as $i = 0, 1, \ldots, N_L$. Further, consider that a given location l_i entered an epidemic state at time t_k, $t = 0, 1, \ldots, T$ if the reproduction number for that location rises above unity for the first time at t_k, where discrete time units represent days based to match the periodicity of official data. This allows us to define a set of events E defined as pairs (l_i, t_k) composed of location and time of each event. Note that events are separated by a spatial distance Δl and a temporal distance Δt, where the spatial distance between two locations can be obtained by means of the application of the Haversine formula to their latitude-longitude coordinates. In turn, we define the temporal distance between two events as the number of days elapsed between them.

We start with a fully disconnected network (composed of only nodes) and proceed to add links between nodes that are temporally close within a maximum allowable distance radius. Thus, links are added when nodes feature spatiotemporal proximity, such that distant nodes are only allowed to connect if they are temporally close to each other. This is aimed at avoiding the indiscriminate addition of links among spatially distant locations. Otherwise, the process would result in a (nearly) fully connected network, in which case the resulting network structure is very little informative. To avoid this, the maximum allowable spatial distance, $d_{\max}$, was initially defined as the distance between Oiapoque and Chuí (4174 km), the largest distance between two locations in Brazil. Then, the maximum allowable distance for the addition of a link was defined as a function of the temporal distance between nodes, given by

$$d\left(\Delta t\right) = \frac{d_{\max}}{1 + \Delta t} \tag{1.5}$$

The resulting network accounts for travel distances and travel times in an integrated way and considers the dynamics of the reproduction number.

1.3 Results

In this section, we present the maps resulting from the reproduction number R_t for each Brazilian municipality. The evolution is traced both by means of the maps and a timeline with a report of the elements that characterized the most representative epidemiological weeks. Next, we present the maps with the maximum value of R_t for each municipality and the network structure formed by cities that entered the epidemic state during up to EW 11, which is symbolic because it preceded the recognition of COVID-19 as a pandemic by the WHO.

1.3.1 Spatiotemporal dynamics of coronavirus spread

Epidemiological week 09. Brazil registered the first case on 26 February 2020. It was a 61-year-old patient who was traveling in Italy from 9 to 21 February. The Ministry of Health reported the first positive case of COVID-19 in the country with mild symptoms and was quarantined at home. The confirmation test was also positive.

Epidemiological week 10. Three state capitals, São Paulo, Rio de Janeiro, and Brasília, present R_t values greater than one, indicating that the threshold for the appearance of the epidemic was reached in these cities. The official data do not feature information on the number of exposed individuals. This information was retrieved using the calibrated SEIR model and from this point it was possible to establish the values of the reproduction number, R_t, in these locations. The data for the next few days confirm the information, since Brazil registered 25

new cases, with a greater number in São Paulo (16) and Rio de Janeiro (3). In the states of Bahia (BA), Alagoas (AL), Minas Gerais (MG), Espírito Santo (ES), and the Federal District (DF) also confirm new cases. The maps show cities that appear with $R_t > 1$, suggesting that the epidemic is already installed. Among them, the capital cities of the states of Amazonas (AM), Pará (PA), Mato Grosso do Sul (MS), Goiás (GO), Paraná (PA), and Rio Grande do Sul (RS). This indicates that the number of cases would increase significantly in these locations in the following days.

Epidemiological week 11. On 11 March, the World Health Organization (WHO) declared the COVID-19 pandemic and declared that the number of infected patients, deaths, and affected countries should increase over the weeks. The Federal District (DF) was the first unit of the federation to establish social distancing measures. By means of a decree, the state governor suspended classes in public and private schools for five days, in addition to events that required licenses from the government of the Federal District. Days later, public services and commercial activities considered nonessential were also suspended, a measure that included restaurants, bars, shops, beauty salons, among others. Similar actions would be taken in the state of São Paulo (SP), on 16 March, and Rio de Janeiro (RJ), on 17 March. The other states also started to take isolation and distancing measures. In a matter of days, the country went from a few dozen confirmed cases to several hundreds. The majority of cases were in the Southeast and Central-West regions. As shown in the map in Fig. 1.4, the reproduction number was higher than one in municipalities in Northern states, such as Roraima (RR), Pará (PA), Amapá (AP), and in the Central-West, such as Mato Grosso (MT) and Mato Grosso do Sul (MS). Two municipalities, one in Mato Grosso do Sul and another in Pará, have $R_t > 3$, which represent high transmission rates.

Epidemiological week 12. On 17 March, the state of São Paulo confirmed the first death in Brazil. At this time, Brazil had 346 confirmed cases of COVID-19. On 18 March, the São Paulo State Department of Health confirmed two more deaths and Brazil reached the total number of 529 confirmed cases. Two days later, on 20 March, the Brazilian Ministry of Health recognized the status of community transmission of the new coronavirus throughout the national territory. On 21 March, the number of deaths in the state of São Paulo rose to 15 and the state governor determined a 15-day quarantine for the 645 municipalities in the state. The government of Roraima (RR) confirmed the first two cases; with this confirmation, all states of the federation had confirmed cases. On 22 March, Brazil already had 1546 confirmed cases and 18 deaths. Municipalities with $R_t > 1$ appeared in all states of Brazil. In the North region, several municipalities have $R_t > 3$, which means that northern states have the highest rate of transmission of the disease at this time. In the Southeast, Northeast, and South regions, the number of municipalities with R_t values greater than one increased. However, for the time being, municipalities with infected people are a minority and appear on the map as isolated points.

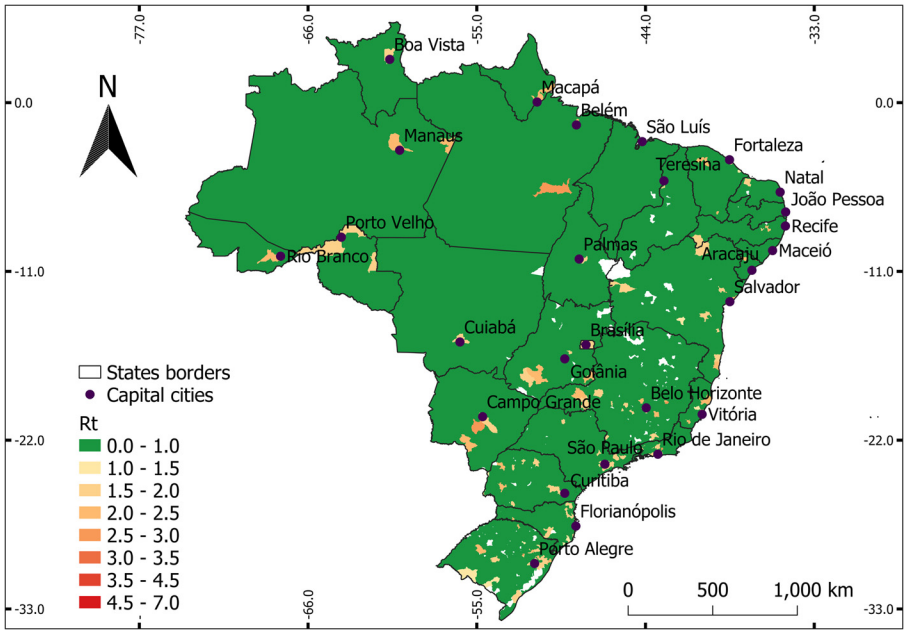

Figure 1.4: Instantaneous reproduction number by the end of week number 11.

Epidemiological week 13. On 24 March, the state of Amazonas had its first death confirmed by COVID-19. And on 29 March, the country already had 4256 confirmed cases and 136 deaths. The leading states: in the North region, the state of Amazonas has 140 confirmed and one death; in the Northeast region, the state of Ceará has 348 confirmed and 5 deaths; in the Midwest region, the Federal District has 289 confirmed cases and one death; in the Southeast region, the state of São Paulo has 1451 confirmed cases and 98 deaths; in the southern region, the state of Rio Grande do Sul has 226 confirmed deaths and two deaths. The map in Fig. 1.5 shows that in the seven-day period, all states have come to a status of accelerated transmission. In the interior of the states, several municipalities with R_t values greater than one appeared, but still as isolated islands. In the states of Amazonas and Pará, R_t values greater than two and three are observed and the beginning of agglomeration of municipalities with accelerated transmission of the disease. This can be also observed in the surroundings of Brasilia, the capital city of Brazil. Considerable growth in the number of municipalities with $R_t > 1$ is observed in the states of the South, Southeast and in the state of Ceará (CE), in the Northeast.

Epidemiological week 14. On 1 April, the Brazilian Health Ministry changes protocols and starts to recommend the use of protective masks to everyone in public places. Due to difficulties in production and import, health authorities suggest the use of cloth models made at home, to attempt to decelerate the fast growth of contamination.

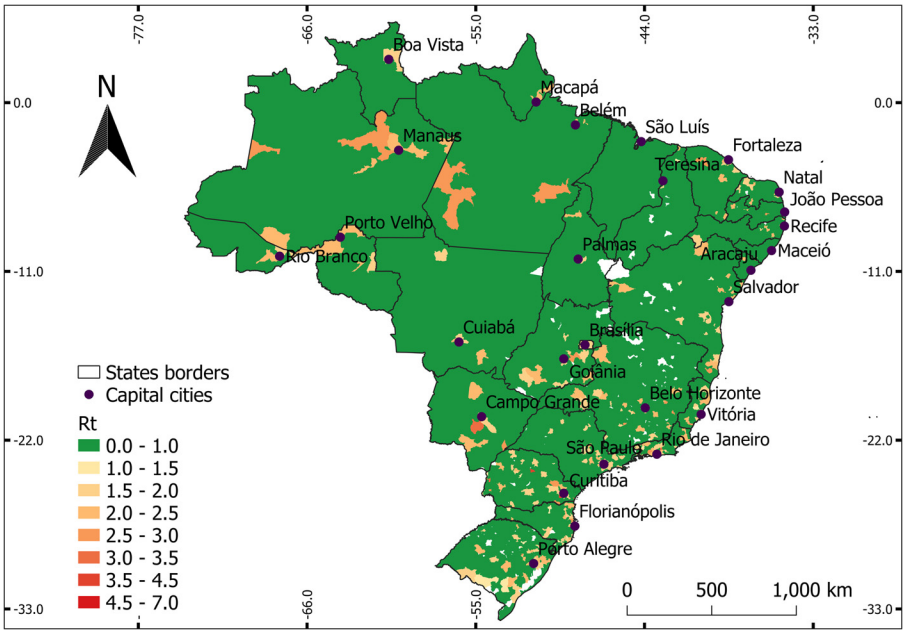

Figure 1.5: Instantaneous reproduction number by the end of epidemiological week number 13.

Epidemiological week 15. The federal government publishes new guidelines on the adoption of differentiated measures regarding social distancing: moving away from Expanded Social Distance (DAS) to Selective Social Distance (DSS). The objective is to promote the gradual return of labor activities without leading to an explosion in the number of cases. On 8 April, the Ministry of Health reported 800 deaths and 15,927 confirmed cases across Brazil. The states of Pernambuco (PE), Amazonas (AM), Bahia (BA) and Ceará (CE) recorded 46, 30, 18, and 53 deaths, respectively. The transmission rates continue to grow in the North and Northeast, and the area covered by viral circulation increases significantly. In the Southeast, the state of São Paulo has the highest number of deaths, with 428, followed by the state of Rio de Janeiro, with nearly a hundred. Four days later, the number of confirmed cases is 22,192 and the number of deaths reached 1223. The states of São Paulo (SP), Amazonas (AM), and Ceará (CE) lead in the number of new cases. There is intense growth in the number of municipalities with $R_t > 1$ throughout Brazil, indicating that the transmission is increasing rapidly. Comparing the maps from EW 13 (Fig. 1.5) and EW 16 (Fig. 1.6), it can be noted that during the period in-between, many neighboring municipalities to those with R_t greater than one acquired a similar or greater level of transmission, demonstrating the transmission between neighboring cities. Orange and dark red spots grew thorough the country. This happened more significantly in the North, where red-shaded islands became agglomerations of municipalities, thus illustrating the short-range transmission between capital cities and interior ones.

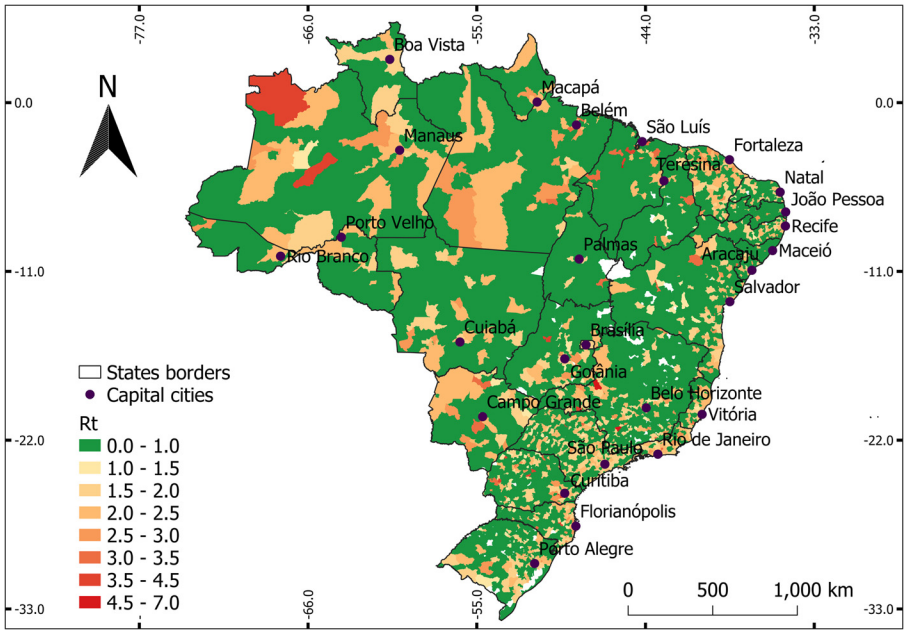

Figure 1.6: Instantaneous reproduction number by the end of epidemiological week number 16.

Epidemiological week 16. In view of the rapid evolution of the epidemic in Brazil and the ineffectiveness of previous actions to contain the spread, the Supreme Federal Court decided that state governments and municipalities can determine their own rules of isolation, quarantine, and restrictions on circulation and transportation. On 16 April, the Brazilian government decides to replace the health minister. As shown in the map in Fig. 1.6, there are outbreaks of the disease across the country, which means that early measures to contain the dissemination did not work. At this time, Roraima state has more intense propagation and $R_t > 1$ values in the range 3 to 4, as shown in Fig. 1.6. This means very rapid transmission is occurring and soon, the state may face increased severity of consequences on the public health system. Clusters of smaller size can be seen in the states of the South and Southeast regions and in Ceará. However, still in most areas of the map, green prevails, which means that most of the municipalities in the country are not facing a state of the epidemic.

Epidemiological week 17. On 23 April, a mayor's decree that required the use of protective masks came into force in the municipality of Rio de Janeiro. Brazil already has over 50 thousand cases and the state of São Paulo (SP) remains the epicenter of the epidemic in the country, concentrating the largest number of deaths. The city of Manaus (AM), in the North of the country, reports hospital and funeral collapse. The morgues no longer support the increased demand and refrigeration containers were installed outside the hospitals to accommodate bodies from deceased COVID-19 patients. The new health minister defends specific guidelines

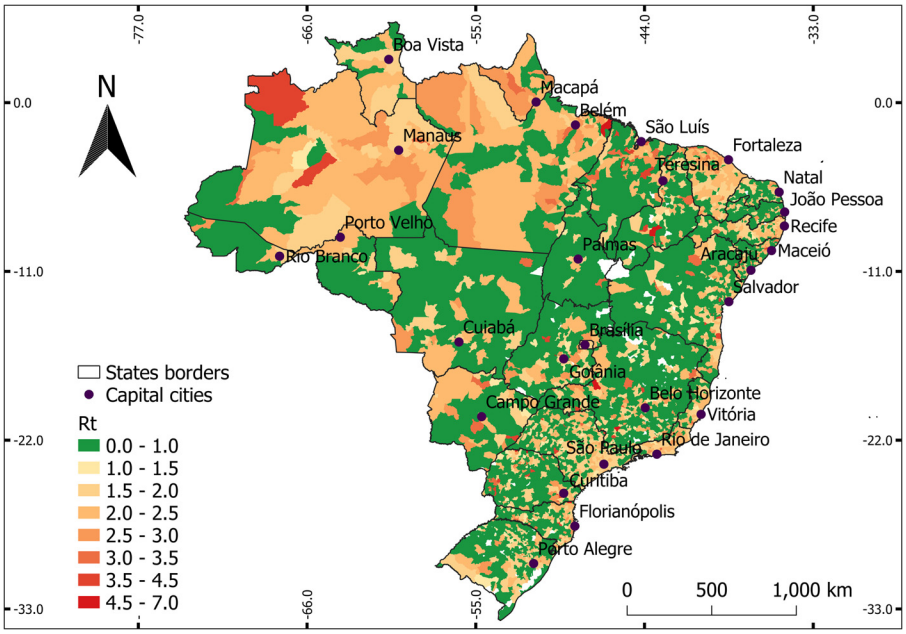

Figure 1.7: Instantaneous reproduction number by the end of epidemiological week number 18.

for each region of the country in view of the heterogeneous way of distribution of cases. In the Northwest region of the country, in Ceará and Pernambuco states, the islands of red-shaded areas became contiguous regions of the same or greater intensity, which means that the epidemic made its way to the interior of the state. The same process occurred in Paraná and São Paulo states, but these states managed to have more controlled transmission intensities. In the Midwest region, agglomerations of municipalities with red-shaded areas appeared in Mato Grosso (MT), Mato Grosso do Sul (MS), and Goiás (GO). Despite having values R_t between 1 and 2, São Paulo remains the epicenter of the epidemic. The growth of cases in the state is also caused by the advance of the disease to the interior cities, coastal cities and Greater São Paulo.

Epidemiological week 18. On 30 April, state justice tribunals decree lockdown in the state of Maranhão (MA) for the duration of ten days, starting on 5 May. The lockdown would be extended to 17 May, by a later decision aimed at giving the state time to enable time to build field hospitals. The decision implicated that the state capital, São Luís, and the cities São José de Ribamar, Paço do Lumiar, and Raposa had to remain closed. The epidemic accelerates in the Northern states with higher values of R_t and larger area covered, as depicted in Fig. 1.7.

Epidemiological week 19. Six states report the collapse of their private health networks: Rio de Janeiro, Ceará, Pernambuco, Amazonas, Maranhão, and Pará no longer have ICU beds

that can be hired by the public network. São Paulo state extends quarantine until 31 May. Rio de Janeiro considers the possibility of decreeing a lockdown throughout the state, with road blocking and circulation restrictions. Brazil has 162,699 confirmed cases and 11,123 deaths. The red-shaded area has grown noticeably in size and intensity in the past two weeks. The Northern region states feature darker shades, indicating acceleration of the transmission rates. Several municipalities with R_t values close to 4 have appeared, indicating very high transmission rates. In the Central-West region, agglomerations of municipalities with high R_t value around the capitals continue to grow. In Rio Grande do Sul state, agglomerations of regions with accelerated transmission are observed in the municipalities along the border with Argentina and Uruguay. The epidemic state hits virtually all coastal cities of Brazil and covers almost the entire area of Northern states.

Epidemiological week 20. On 5 May, the government of Pará decreed the state of lockdown in the metropolitan region of Belém, severely restricting the circulation of citizens. On 11 May, a decree by the Brazilian president includes industrial activities, civil construction and beauty salons, gyms, and barbershops in the list of essential activities. Such measure significantly increases the number of businesses allowed to function during the period of the pandemic. On 13 May, the new health minister resigns and is replaced by interim minister general Eduardo Pazuello, who changes the protocols for the application of chloroquine and hydroxychloroquine in the country. During the period, the World Health Organization (WHO) reinforces that the use of drugs in this context causes more side effects than benefits. The map in Fig. 1.8 shows that the viral circulation continues to grow, and an increasing number of municipalities enter an accelerated transmission regimes, several of them with high transmission rates, with R_t values around 4. In North, Northeast, and Southeast regions, there are few municipalities without confirmed cases.

Epidemiological week 21. On 24 May, Brazil has 363,618 confirmed cases and 22,716 deaths. In South region, the most serious situation is in Paraná state. In Rio Grande do Sul state, agglomerations of municipalities with disease grew larger in areas, albeit with mild values of R_t. On 25 May, the lockdown period in the metropolitan region of Belém, the capital city of Pará, is terminated.

Epidemiological week 22. The government of São Paulo state announces a plan to reopen the economy. Gradual resumption is to happen in regions that have a reduction in the number of cases, availability of hospital beds, and obedience to social distancing measures. Although the epidemic in the country is accelerating, capitals such as São Paulo, Rio de Janeiro, Fortaleza, and Manaus plan to reopen economic activities as of 1 June as the transmission rates are receding in these cities. However, the four states are the most critical. São Paulo is the leader in cases and deaths; Rio de Janeiro has about 50,000 confirmed cases of coronavirus, with an explosion of deaths in May. Ceará is the third state in cases and deaths, and becomes the epicenter of the disease in the Northeast. Amazonas has already suffered a collapse of the health

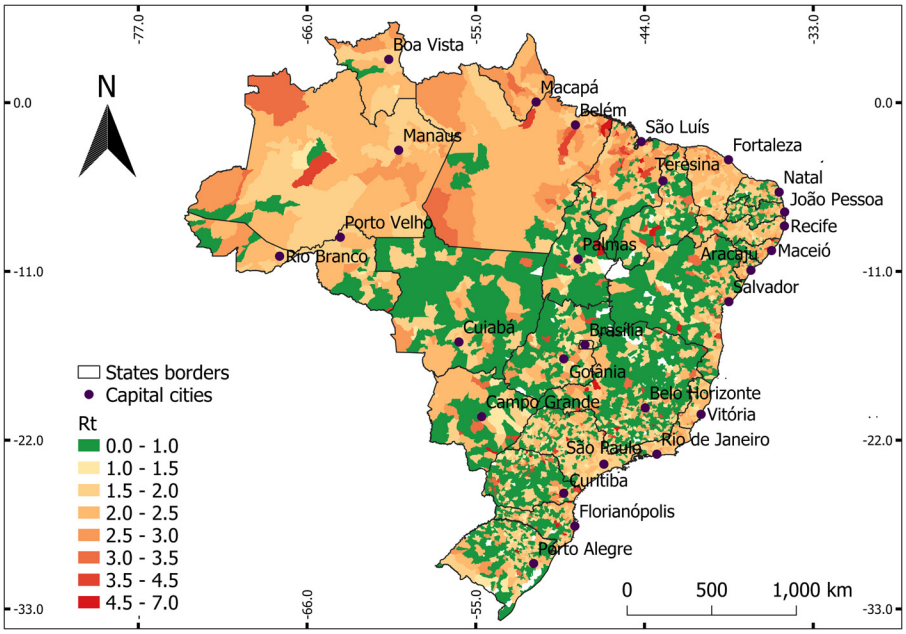

Figure 1.8: Instantaneous reproduction number by the end of epidemiological week number 20.

system and is fourth in the ranking of confirmed cases and deaths. Only more remote areas of the country remain with $R_t < 1$, as shown in Fig. 1.9.

Epidemiological week 23. The easing of restrictions occurs in several cities, and the Pan American Health Organization (PAHO) recommends caution because it assesses that an eventual second wave of contamination can put efforts made at risk. At that time, Brazil had 691,962 confirmed cases and 36,499 deaths.

Epidemiological week 24. The map in Fig. 1.10 shows that in the period of 14 days, the disease has progressed in Brazil, covering almost the entire territory. Municipalities not in the epidemic state (green in the map) are small islands. In the states of Pará, Mato Grosso, Mato Grosso do Sul, and Tocantins, dark red spots are observed with levels of R_t values around 4. After reaching the peak of transmission in May, the states in the North see the transmission rates receded. Some municipalities even have decelerated R_t to values lower than the unit, thus having suppressed the conditions for the maintenance of the epidemic state.

Epidemiological week 26. The map in Fig. 1.11 shows that in the period of 14 days, agglomerations of municipalities with $R_t < 1$ (green areas on the map) emerged in the North region, which indicates that the transmission rates are receding. In the rest of the country, the transmission levels remain high, but it seems that the peak of the first wave has been reached. In

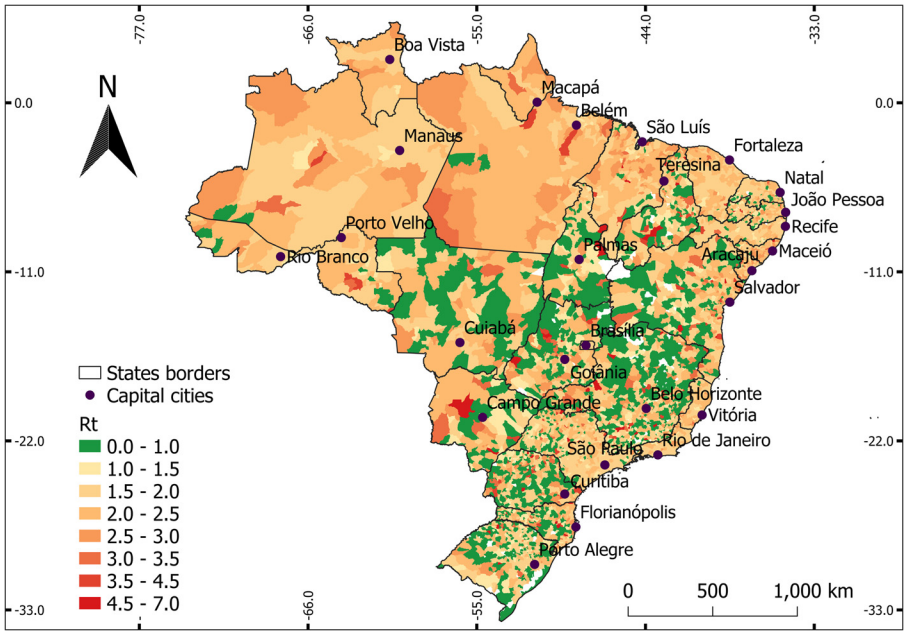

Figure 1.9: Instantaneous reproduction number by the end of epidemiological week number 22.

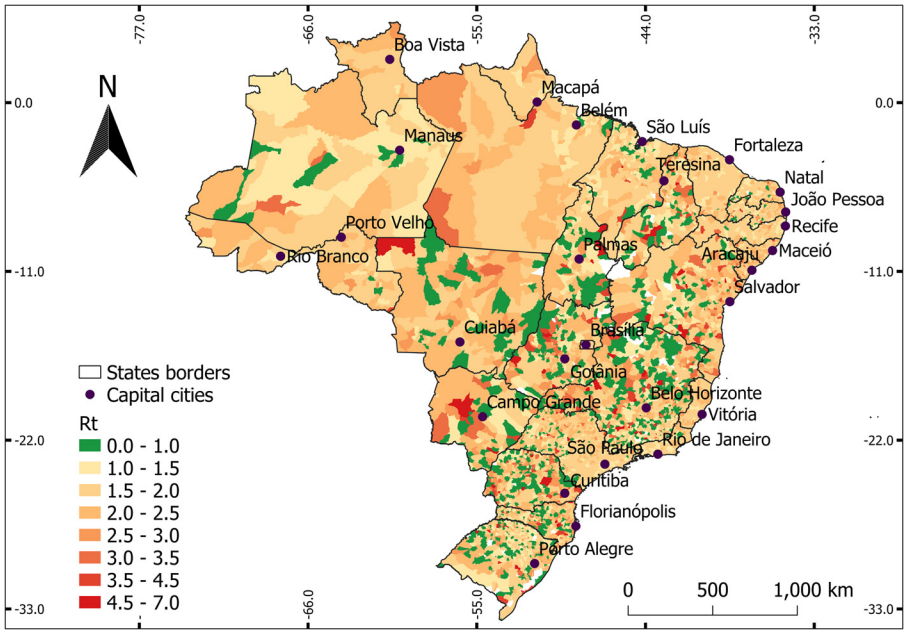

Figure 1.10: Instantaneous reproduction number by the end of epidemiological week number 24.

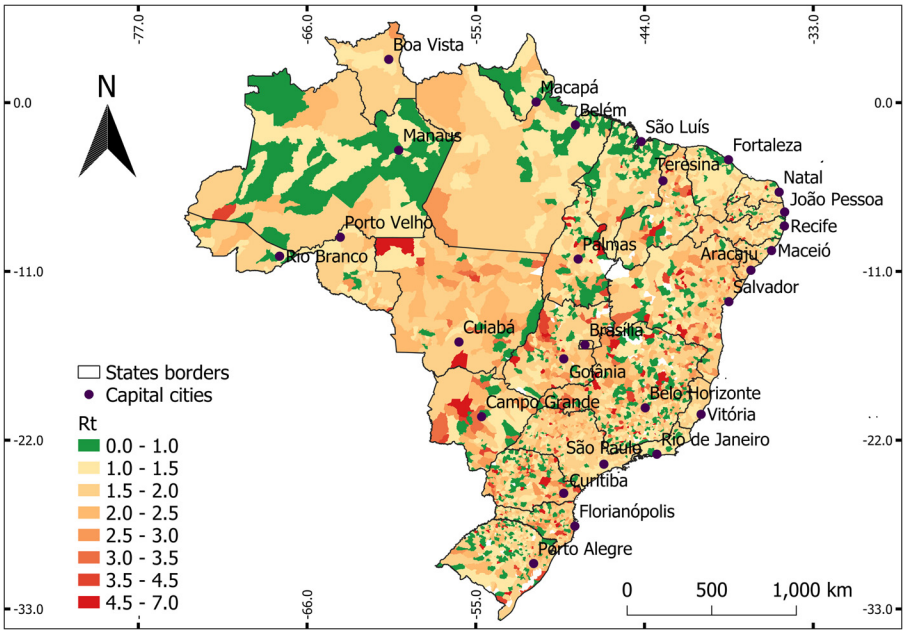

Figure 1.11: Instantaneous reproduction number by the end of epidemiological week number 26.

the states of Pará, Mato Grosso, Mato Grosso do Sul, and Tocantins, there are dark red spots that mean that the levels of R_t increased to values around 4. The number of smaller sized dark spots also increased in the states of the Northeast, Southeast, and South. At the time, the country has the highest daily number of deaths since the beginning of the epidemic, and it has surpassed the United States and the United Kingdom in total deaths. The number of deaths in São Paulo state continues to increase rapidly, hitting new highs daily. Despite of the scenario, the state government announces the resumption of classes and the continuity of the process of reopening the economy due to strong concerns about the financial health of businesses.

Epidemiological week 28. Brazil has overcome 1.6 million confirmed cases and 65,000 deaths. The map in Fig. 1.12 shows that the epidemic recedes in most Northern states and around capital cities of the Northeast, which were among the first ones to face epidemic states. The rate of new infections recedes but there may still be an increase in the number of confirmed and deaths. In Northeast, the effects of the epidemic are still strong in Bahia, Pernambuco, and Ceará, although the transmission rates have decreased as well. The darker shades of red in Mato Grosso, in the Central-West region, indicate that the epidemic is accelerating in the region. Several municipalities are observed with R_t values around 4.

Epidemiological week 29. Brazil reaches the mark of 2.1 million confirmed cases and 80 thousand deaths. The leading state in the number of cases in the North is Pará, which has

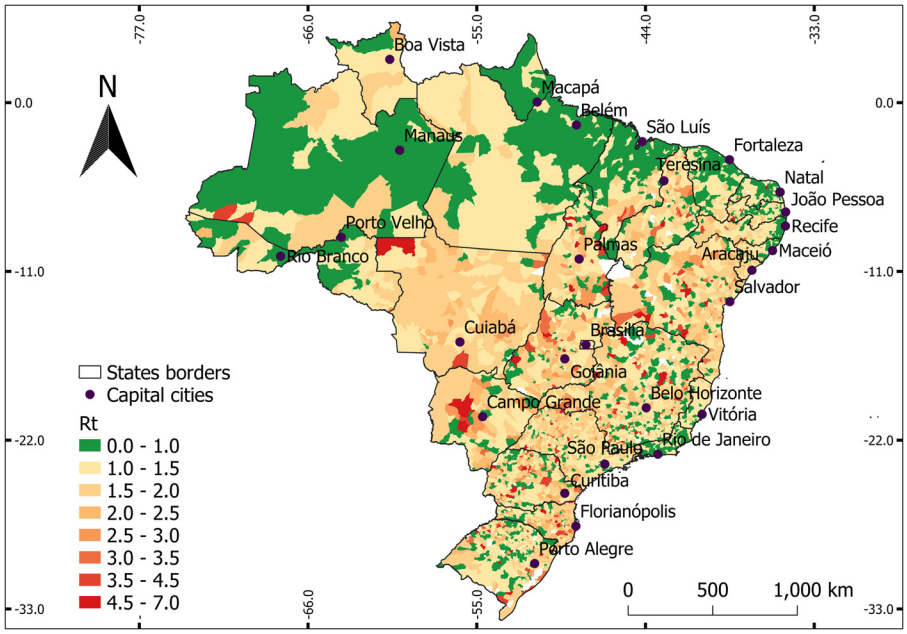

Figure 1.12: Instantaneous reproduction number by the end of epidemiological week number 28.

137,484 confirmed cases and 5523 deaths; in Northeast, the state of Ceará, which has 146,972 confirmed cases and 7178 deaths; in Central-West, the Federal District has 82,420 confirmed cases and 1085 deaths; in the Southeast region the state of São Paulo has 415,049 confirmed cases and 19,732 deaths; in the South region, the state of Paraná has 54,629 confirmed cases and 1325 deaths. The map in Fig. 1.13 shows relaxation of transmission in Brazil, particularly in the North, Northeast, and Southeast regions. In the North region, the epidemics continue to recede, as well as in the Northeast, and large areas with $R_t < 1$ (green color) appeared. The majority of municipalities in the South and Southeast regions have decreasing levels of R_t, which remain slightly higher than one but are receding relatively to previous weeks.

Epidemiological week 31. Brazil has 2.7 million confirmed cases and 94,130 deaths. The map in Fig. 1.14 shows that in the North region most municipalities appear with $R_t < 1$, indicating that the first wave of the epidemic continues to recede in the region. Tocantins is the only state of the North region where most municipalities have $R_t > 1$. Most agglomerations of municipalities with $R_t > 1$ are located in the Central-West region, in the states of Mato Grosso, Mato Grosso do Sul, and Goias. In the Northeast region, the states of Ceará, Bahia, and Pernambuco, the epidemic continues to recede. The South and Southeast regions still have several municipalities with shades of red, particularly in the innermost areas of the states. In general, the transmission of COVID-19 in Brazil has decreased considerably. The daily number of new infected stabilized and starts to present a decline trend.

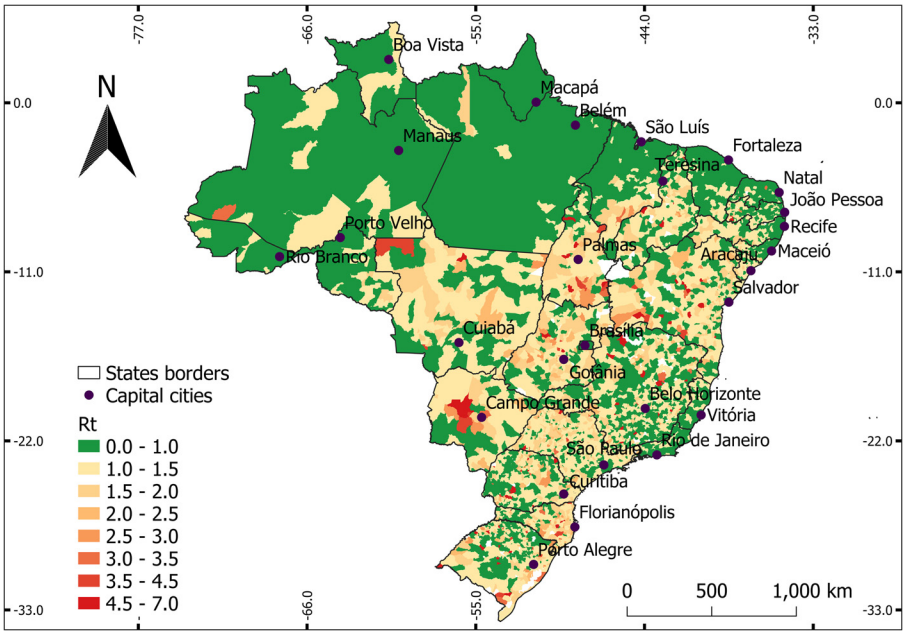

Figure 1.13: Instantaneous reproduction number by the end of epidemiological week number 30.

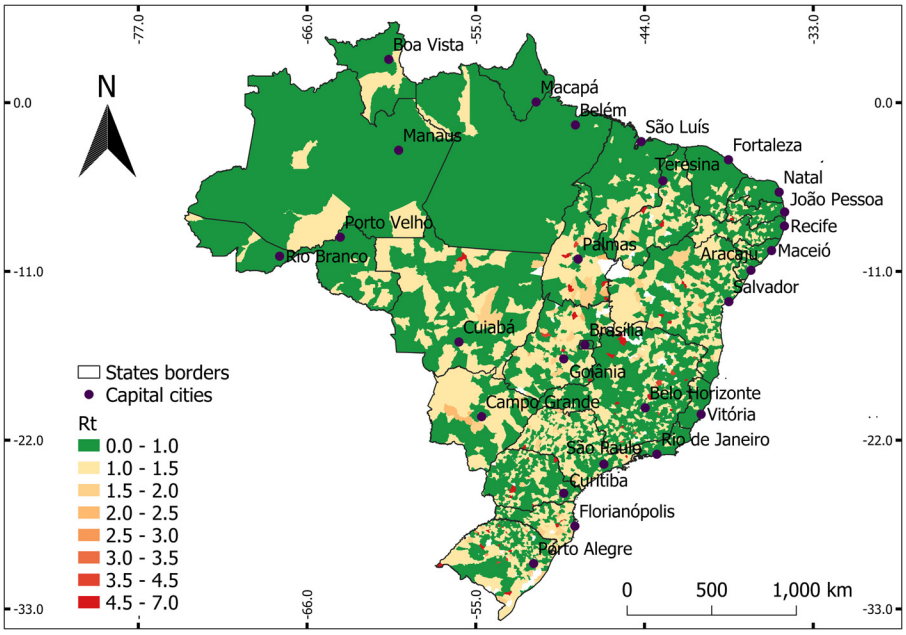

Figure 1.14: Instantaneous reproduction number by the end of epidemiological week number 32.

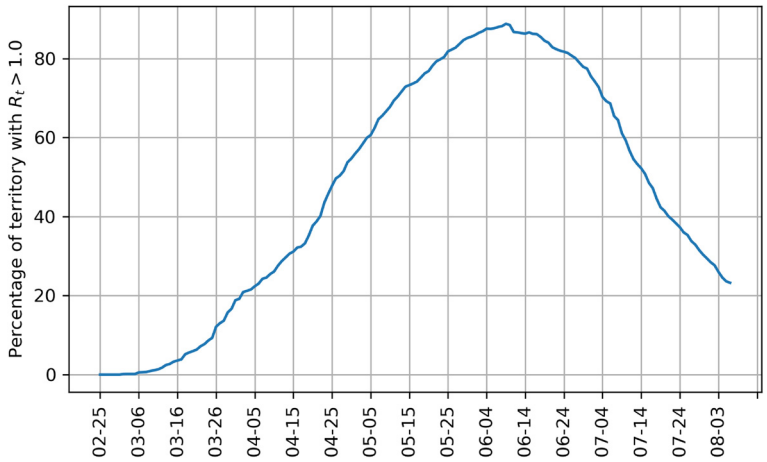

Figure 1.15: Percentage of the Brazilian territory with accelerated transmission dynamics ($R_t > 1$).

By the end of epidemiological week 32, the number of active cases is about 744,644 and presents a tendency to decline. This fact, allied with a low reproduction number in most regions of the country, shall result in declining levels of hospitalizations and stabilization in the number of daily deaths, followed by monotone decline of both in the following months. It seems that the first wave of the epidemic in Brazil has come to an end.

1.3.2 Coronavirus spread and area coverage of the epidemic

From the maps above, it can be identified that the peak of area coverage in terms of cities with accelerated transmission dynamics occurred between epidemiological weeks 24 and 25. The spatial coverage of cities in ongoing epidemic state, $R_t > 1$ had rapid growth since February, reaching the peak of about 90% of the area of the country in mid-June, as shown in Fig. 1.15. From that time on, the coverage of the epidemic state receded to the point that in the beginning of epidemiological week 32 there is about 20% of the country area covered by cities with accelerated transmission.

Regarding the transmission velocity, Fig. 1.16 shows the maximum reproduction number observed in each municipality. From this figure, it is noticeable that the state of São Paulo, which has one of the highest demographic densities in Brazil (see Fig. 1.2a) and has the largest air transport hub in the country (see Fig. 1.3), managed to keep the reproduction number relatively low along the period, with maximum values in the interval $[1, 2]$ in most areas.

In Fig. 1.17 we present the network structure formed by the municipalities that entered the epidemic state in the weeks following the first reported case in Brazil. It can be observed that

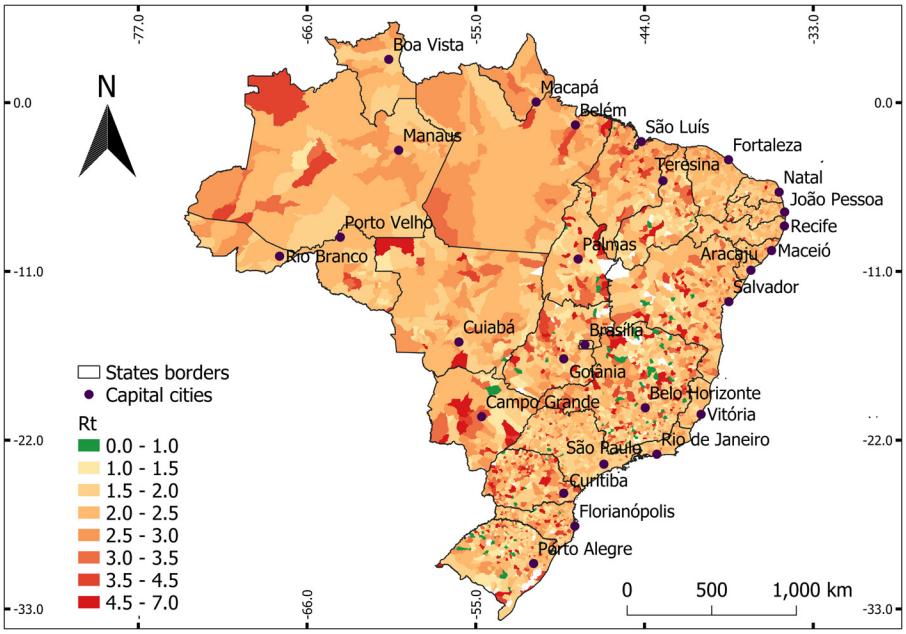

Figure 1.16: Maximum reproduction number in each municipality during the first wave of the epidemic.

the nodes participating in the network structure (in red) are hubs of air transportation of passengers, according to the description provided in Fig. 1.3. The result indicates that the initial contagion pathways are mainly composed of air links between state capitals. In addition, the large distances covered by contagion in a matter of a few days indicate that the air transport network might have been a major early contributor to the spread of the pandemic.

Following the spread of the contagion among the air transportation network, the circulation of the virus reached interior cities in the following weeks, supposedly by means of road transportation.

1.4 Discussion

1.4.1 Early spread of coronavirus in Brazil

The initial network structure of cities that entered the epidemic state in Brazil during EW 10 and EW 11, as shown in Fig. 1.17 indicates that the air transport network might have had a central role in the rapid spread of coronavirus in the country. The maps of the evolution of the epidemic state show the cities featuring main air transport hubs entered the epidemic state first. This indicates that the adoption of social distancing measures and improved hygiene and

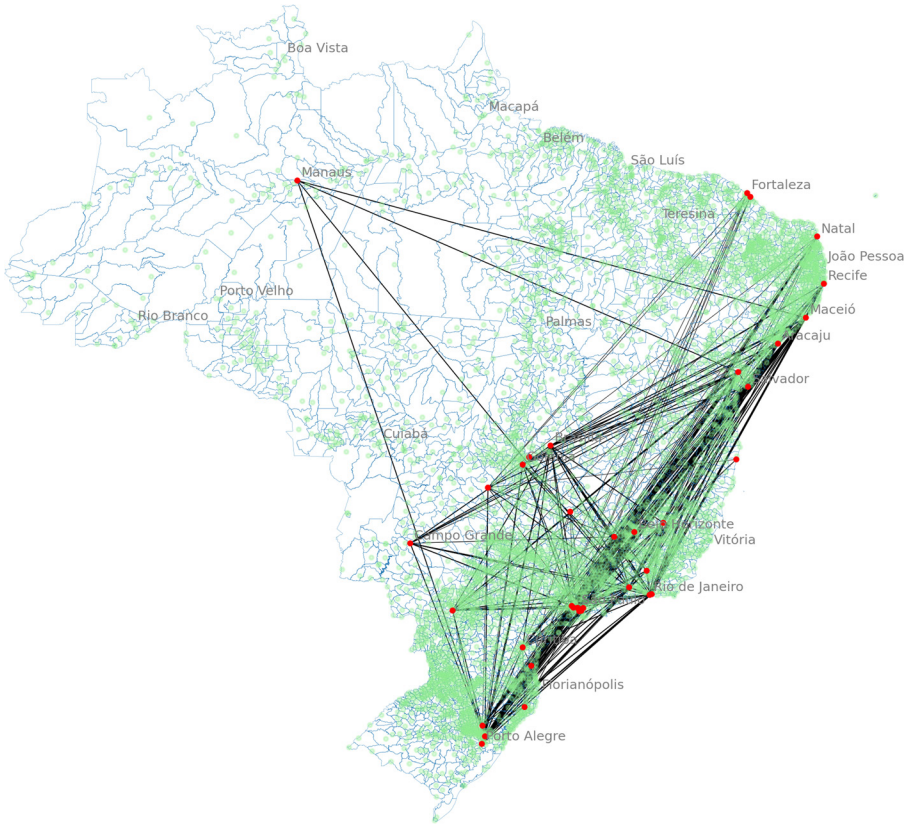

Figure 1.17: Network structure showing links between cities that first entered the epidemic state: nodes correspond to cities with $R_t > 1$ during EW 10 and EW 11, and edge widths represent the temporal distance between two connected nodes, being thicker edges the ones representing the least temporal distance.

disinfection measures in airport environments came around late enough to allow widespread development of contagion.

Another point, as it can be seen from visual inspection of Fig. 1.17, this widespread contagion network was already formed when the WHO declared COVID-19 as a pandemic. This illustrates the importance of studying the epidemics on the basis of its reproduction number, R_t, instead of regarding only the number of confirmed cases as a basis for decision-making. The reproduction number offers a clearer basis for prognostic since it holds the most influential piece of knowledge about the dynamical behavior of an epidemic, irrespective of the model under consideration.

Since the results indicated that the air transport network played an important role in the rapid spread of the disease internally, it remains a task for air transport regulatory agencies to elaborate more agile and effective protocols that help suppress the contagion in early stages of future epidemics with similar transmission characteristics.

1.4.2 Spread velocity

The network structure formed by municipalities in an epidemic state two weeks after the first case was reported in Brazil, shown in Fig. 1.17, indicates that the initial spread velocity of the virus in Brazil was high in the sense that the viral circulation reached very distant locations in a very short time. As one recalls that in the first two weeks the coronavirus circulation had not been declared a pandemic by the WHO and the use of masks had not yet been recommended by Brazilian Health Ministry, it now seems that both these measures came late enough to allow the early spread of the virus through the country. This allowed the epidemic to form the initial contagion network that would later spread further to interior and most remote regions.

The spread velocity was high in terms of area coverage until mid-June, as shown in Fig. 1.15 and Fig. 1.16. Later, as the epidemic state began to progressively recede in the North, Northeast, and Southeast, the first wave of the epidemic remained strong in the Midwest and South, where it took longer to spread and develop.

1.4.3 Brazil's failure in containing the pandemic at early stages

The network of municipalities in epidemic state formed up to EW 11 (Fig. 1.17) in Brazil (and thus before the WHO declared COVID-19 as a pandemic) indicates that early containment strategies were unsuccessful. Indeed, Candido et al. [20] studied the influx of passengers from countries with reported COVID-19 outbreaks by EW 10, having estimated that about 54.8, 9.3, and 8.3% of all imported cases originated from infected travelers flying to Brazil from Italy, China, and France, respectively. A later study by Candido et al. [19] that applied phylogenetic analysis suggested that community transmission in Brazil dates to early March. This shows that the recognition of community transmission by the Health Ministry, issued on 20 March, was at least two weeks late. As observed by Candido et al. [19], the restrictions on international travels implemented after this have limited impact.

1.5 Final remarks

This study provided valuable information regarding the likely pathways of contagion in Brazil. This information can be applied in practice to counteract the spread by means of hygiene and social distancing protocols upon the occurrence of another epidemic with similar

transmission characteristics. The results also indicate that important early measures by the WHO and Brazilian Health Ministry were late in the sense that they were not timely enough to avoid the formation of a network of areas in an epidemic state throughout the country. This initial network setup supposedly managed to spread from larger cities that hold air transport hubs to interior and remote areas in the following days.

The careful examination of the results by public health authorities may help evaluate their social distancing policies both in terms of timeliness and effectiveness by means of a retrospective analysis that may enhance the prospect of strategies and promptness upon future demands upon public health.

References

[1] N. Ferguson, D. Laydon, G. Nedjati-Gilani, et al., Report 9: Impact of the non-pharmaceutical interventions (NPIs) to reduce COVID-19 mortality and healthcare demand, 2020.
[2] S. Flaxman, S. Mishra, A. Gandy, H. Unwin, et al., Estimating the effects of non-pharmaceutical interventions on COVID-19 in Europe, Nature 584 (2020) 257–261.
[3] C. You, Y. Deng, W. Hu, et al., Estimation of the time-varying reproduction number of COVID-19 outbreak in China, International Journal of Hygiene and Environmental Health 228 (2020) 113555.
[4] H.W. Hethcote, Three Basic Epidemiological Models, in: Applied Mathematical Ecology, in: Biomathematics, Springer, Berlin, 1989, pp. 119–144.
[5] O. Diekmann, J.A.P. Heesterbeek, J.A.J. Metz, On the definition and the computation of the basic reproduction ration R0 in models for infectious diseases in heterogeneous populations, Journal of Mathematical Biology 28 (1990) 365–382.
[6] W.O. Kermack, A.G. McKendrick, Contributions to the mathematical theory of epidemics-I, Bulletin of Mathematical Biology 53 (1991) 33–55.
[7] W.O. Kermack, A.G. McKendrick, Contributions to the mathematical theory of epidemics-II. The problem of endemicity, Bulletin of Mathematical Biology 53 (1991) 57–87.
[8] W.O. Kermack, A.G. McKendrick, Contributions to the mathematical theory of epidemics-III. Further studies of the problem of endemicity, Bulletin of Mathematical Biology 53 (1991) 89–118.
[9] H.W. Hethcote, The mathematics of infectious diseases, SIAM Review 42 (2000) 599–653.
[10] S.M. O'Regan, T.C. Kelly, A. Korobeinikov, et al., Lyapunov functions for SIR and SIRS epidemic models, Applied Mathematics Letters 23 (4) (2010) 446–448.
[11] Cruz Vargas-De-Leon, On the global stability of SIS, SIR and SIRS epidemic models with standard incidence, Chaos, Solitons and Fractals 44 (12) (2011) 1106–1110.
[12] Drew Posny, Jin Wang, Computing the basic reproductive numbers for epidemiological models in nonhomogeneous environments, Applied Mathematics and Computation 242 (2014) 473–490.
[13] W.C. Roda, M.B. Varughese, D. Han, et al., Why is it difficult to accurately predict the COVID-19 epidemic?, Infectious Disease Modelling 5 (2020) 271–281.
[14] R.N. Thompson, J.E. Stockwin, R.D. van Gaalen, et al., Improved inference of time-varying reproduction numbers during infectious disease outbreaks, Epidemics 29 (2019) 100356.
[15] N. Chen, M. Zhou, X. Dong, et al., Phase-adjusted estimation of the number of Coronavirus Disease 2019 cases in Wuhan, China, Cell Discovery 6 (2020).
[16] T. Liu, J. Hu, J. Xiao, et al., Time-varying transmission dynamics of novel coronavirus pneumonia in China, bioRxiv, https://doi.org/10.1101/2020.01.25.919787, 2020.

[17] J.M.V. Grzybowski, R.V. da Silva, M. Rafikov, Expanded SEIRCQ model applied to COVID-19 epidemic control strategy design and medical infra-structure planning, Mathematical Problems in Engineering 1 (2020) 1–21.
[18] Leonardo R. López, Xavier Rodó, A modified SEIR model to predict the COVID-19 outbreak in Spain and Italy: simulating control scenarios and multi-scale epidemics, preprints with The Lancet, 2020.
[19] D.D.S. Candido, A. Watts, L. Abade, et al., Routes for COVID-19 importation in Brazil, Journal of Travel Medicine 27 (2020).
[20] D.S. Candido, I.M. Claro, J.G. de Jesus, et al., Evolution and epidemic spread of Sars-cov-2 in Brazil, Science 369 (2020) 1255–1260.
[21] Q. Li, X. Guan, P. Wu, et al., Early transmission dynamics in Wuhan, China, of novel coronavirus-infected pneumonia, The New England Journal of Medicine 382 (2020) 1199–1207.
[22] NCID, National Centre for Infectious Diseases. Position statement from the National Centre for Infectious Diseases, 2020.
[23] IBGE, Territorial Areas, Territorial area - Brazil, Major Regions, Federation Units and Municipalities, 2020.
[24] The World Bank, Total population, United Nations Population Division. World Population Prospects: 2019 Revision, 2019.
[25] IBGE, Estimativa da população residente para os municípios e para as unidades da federação brasileiros com data de referência em 1° de julho de 2017, Instituto Brasileiro de Geografia e Estatística - IBGE, 2017.
[26] The World Bank, GDP (current US$), World Bank national accounts data, and OECD National Accounts data files, 2019.
[27] The World Bank, GDP per capita (current US$), World Bank national accounts data, and OECD National Accounts data files 2019.
[28] UNDP, 2019 Human Development Index Ranking, Human Development Reports, 2019.
[29] UNDP, FJP, and IPEA, O Índice de Desenvolvimento Humano Municipal Brasileiro: Atlas do desenvolvimento humano no Brasil, PNUD (2013) 96.
[30] The World Bank, Air transport, passengers carried, International Civil Aviation Organization, Civil Aviation Statistics of the World and ICAO staff estimates, 2018.
[31] IBGE, Air Links, The 2010 Air Links, 2010.
[32] Brasil.io, COVID-19, 2020.